ISET Journal of Earthquake Technology, Paper No. 601, Vol. 62, No. 3, September 2025, pp. 165-179

SEISMIC PERFORMANCE OF FIXED-BOTTOM AND FLOATING OFFSHORE WIND TURBINES

Upasana Nath
Doctoral Research Scholar, Department of Civil Engineering, School of Infrastructure
Indian Institute of Technology Bhubaneswar, Odisha-752050, India, Email id: un13@iitbbs.ac.in

Maria James
Doctoral Research Scholar, Department of Civil Engineering, School of Infrastructure
Indian Institute of Technology Bhubaneswar, Odisha-752050, India, Email id: a21ce09004@iitbbs.ac.in

Sumanta Haldar*
Professor, Department of Civil Engineering, School of Infrastructure
Indian Institute of Technology Bhubaneswar, Odisha 752050, India, Email id: sumanta@iitbbs.ac.in

ABSTRACT

This study evaluates the seismic performance of offshore wind turbines (OWTs) under bi-directional earthquake loading, focusing on both fixed-bottom and floating structures. For fixed-bottom OWTs, time-history analyses were conducted to assess dynamic responses of jacket supported OWTs considering two horizontal seismic components. The results were compared to those obtained using the percentage combination rules (30% and 40%) from building codes. It was found that the 30% combination rule reasonably predicts tower top displacement and rotation, with differences of 3% to 25% compared to time-history analysis. Additionally, a fragility analysis of jacketed OWTs was performed to evaluate seismic vulnerability under different damage states based on serviceability and ultimate limit states. The results show that tower-top drift is more vulnerable in the serviceability limit state compared to the ultimate limit state, particularly for low to high levels of earthquake intensity. For floating wind turbines, the study performed a coupled multi-directional seismic analysis of a Tension Leg Platform (TLP) wind turbine. TLPs were found to be highly susceptible to pulse-like ground motions, mainly due to large velocity pulses. Additionally, the variability in responses increased with peak ground acceleration, highlighting the need for larger safety margins in high seismic risk areas. Seismic vulnerability assessments indicate that jacket structures exhibit higher susceptibility to seismic shaking compared to Tension Leg Platform (TLP) floating wind turbines. The study provides valuable insights for improving the seismic design of OWTs, offering targeted risk mitigation strategies to enhance safety and structural resilience in earthquake-prone regions.

KEYWORDS: Fragility analysis; Ground motion directionality; Incremental dynamic analysis; Jacket; Offshore wind turbine; Percentage combination rule; TLP

INTRODUCTION

In recent years, wind energy has emerged as one of the most promising sources of renewable energy, offering a viable replacement for conventional fossil fuels. The installed global offshore wind capacity reaches 75.2 GW in 2023, with an ambitious target set to reach 487 GW by the end of 2033 (GWEC, 2023). The United Kingdom, Germany, China, Denmark, the Netherlands, Belgium, the United States, and Sweden (Majid, 2020) are the main investors of offshore wind energy. India with large area under exclusive economic zone, offers greater potential to explore and utilize offshore wind farms. Tamil Nadu and Gujarat are identified as the most feasible locations with an available wind energy potential of 70 (total capacity) GW at 100–125 m hub height (NIWE) with an initial target set to 30 GW by 2030. The bathymetry profile along with feasible locations for fixed (NIWE, 2018) and floating wind turbines (James and Haldar, 2024) are presented in Figure 1. The large shelf water within the proximity of coastline along with a high wind energy potential (Figure 2) makes these locations most feasible for offshore wind farm. In Gujarat, monopile and jacket foundations are the most recommended for shallow water depths, while floating wind turbines may offer a viable alternative for deep and complex seabed conditions near Dwarka, Porbandar, and Veraval along the Gujarat coast. On the other side, for Tamil Nadu, monopile foundations are the most

https://doi.org/10.63898/XWWZ9524
*Corresponding Author

suitable option due to stronger winds in the shelf water regions, where depths are less than 30 meters. Jacket is also a viable option while, the sudden abrupt change in the bathymetry profile suggest limited potential for the deployment of floating wind turbines (cf. Figure. 1).

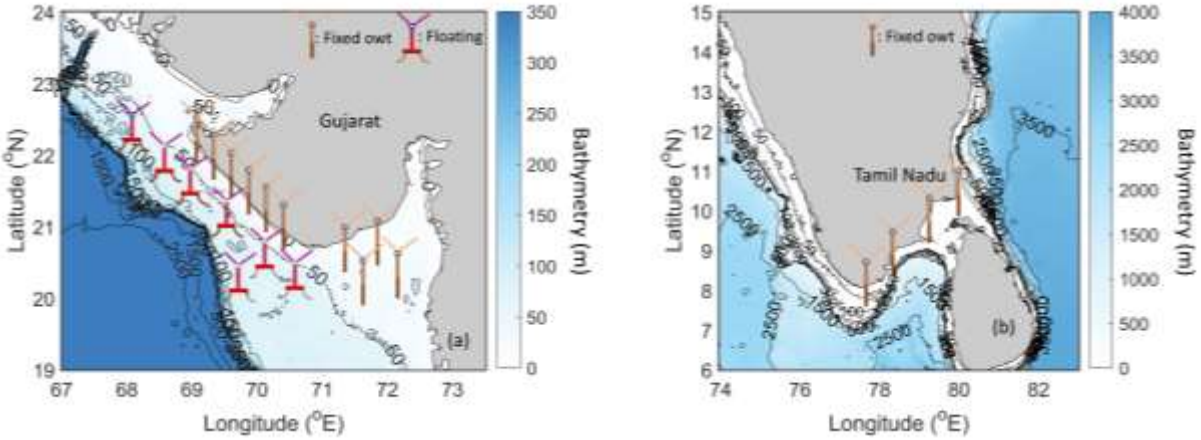

Fig. 1 Feasible Locations for the deployment of offshore wind turbine along the Indian coast of (a) Gujarat (adapted from James and Haldar, 2024) (b) Tamil Nadu

Indian offshore regions are characterized by seismic activity with peak ground accelerations (PGA) ranging from 0.1g to 0.36 g, particularly along the west coast. Gujarat is classified under Seismic Zone V, the highest risk category for earthquakes in India. The region experiences frequent high-magnitude earthquakes due to tectonic movement in which Indo-Australian tectonic plates slides under Eurasian plate. The Kachchh (Kutch) Rift Basin is the most active seismic zone, with major faults like the Kachchh Mainland Fault (KMF), Katrol Hill Fault (KHF), and South Wagad Fault (SWF). The Narmada-Son Fault (NSF), running across southern Gujarat, adds to the seismic risk in the state. 1819 Rann of Kutch earthquake along the Allah Bund Fault with Magnitude of 7.8, Anjar earthquake of magnitude 6.1 near Katrol Hill Fault and Bhuj earthquake of 2000 near the Kachchh Mainland fault with a magnitude of 7.7 are the major historical earthquakes happened in these regions. On the other side, Tamil Nadu experiences lower seismicity compared to Gujarat with a few ancient faults and some neotectonics that could lead to localized earthquakes. The Palghat-Cauvery Shear Zone is a significant neotectonics in the southern part of the state, contributing to minor seismic events. The Eastern Ghat Boundary Fault runs along the state's eastern coast, is also influencing the tectonics of the region. Figure 2 presents the seismic hazard map and annual mean wind speed distribution for Gujarat and Tamil Nadu. Scatter plots show earthquake occurrences with magnitudes greater than 4 in these regions from 1900 to the present. Earthquakes are predominantly concentrated in the Kutch region of Gujarat, indicating higher seismic intensity, while Tamil Nadu has experienced relatively few significant earthquakes over the past century. In addition to ground shaking and fault rupture, the Gujarat coastal seabed is covered by 5–10 meters of coastal sand deposits, underlain by silty clay layers, making the region susceptible to liquefaction.

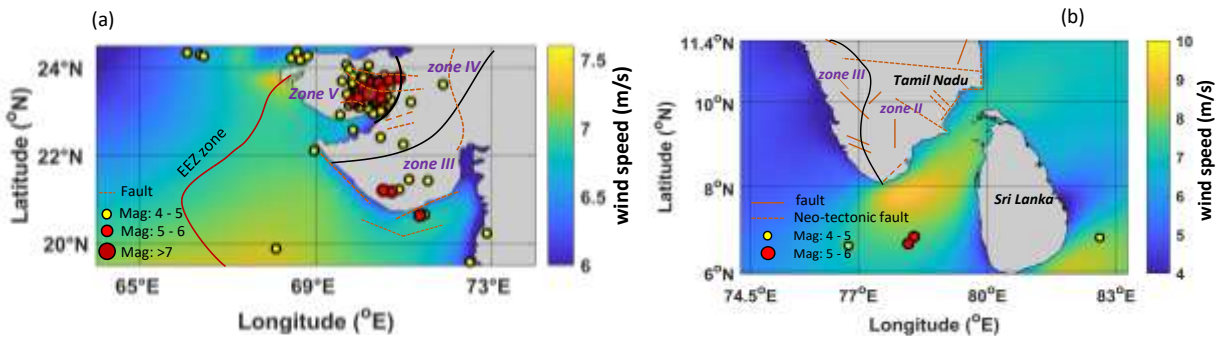

Fig. 2 The distribution of annual mean wind speed and seismic hazard map including fault planes along the coast of Gujarat and Tamil Nadu

Current design guidelines and codes such as IEC 614000-3 (2009), Germanischer Lloyd (2010), and DNV-OS-J101 (2014) suggest to consider the seismic loads in account but no specific design guidelines are recommended to evaluate the seismic performance of the offshore wind turbines (OWTs). The literature on the seismic behaviour of OWTs is less extensive compared to that of onshore wind turbines (Hovind et al. 2014; Katsanos et al. 2016). However, some studies have emphasized the importance of considering seismic loading in the design of these structures (Wang and Dong 2011; Prowell et al., 2014; Kim et al., 2014; Patil et al., 2016; De Risi et al., 2018; Kaynia 2019; Patra and Haldar 2020; Patra and Haldar 2021a; Patra and Haldar 2021b); James and Haldar, 2022). Alati et al. (2015) performed a seismic analysis of a 5 MW jacket-supported OWT under three different load cases. The study indicated that earthquake loading induces significant stress demand even at a moderate peak ground acceleration (PGA) level. Zheng et al. (2015) reported the combined effect of seismic and wave load on OWTs by conducting a scale model test. James and Haldar (2022) analyzed the effect of seismic loading combined with wind, wave, and current loading for a 10 MW jacket-supported OWT concluding that considerable amplification of acceleration occurs due to the vertical component of seismic motion. De Risi et al. (2018) conducted a vulnerability study of monopile-supported offshore wind turbines using unscaled natural earthquakes. This study demonstrated that the strong crustal and interface earthquakes caused vulnerable damage to the OWT.

Numerous studies have been conducted to examine the influence of ground motion directionality on the seismic behaviour of building frames and bridge piers (Kalkan and Kwong 2013; Athanatopoulou 2005; Basu and Shinozuka 2011). However, a limited number of studies have demonstrated the influence of ground motion directionality on the dynamic responses OWTs (Wang and Dong 2011; Sharmin et al. 2017; Tran et al. 2020; Nath and Haldar 2024). Tran et al. (2020) investigated the seismic demands of a 5 MW fixed jacket-supported OWT increase at other angles of incidence compared to 0^{o} angle of orientation. Mo et al. (2021) examined the effect of ground motion direction on the seismic dynamic responses of monopile supported OWT and the results imply that using of the standard input in the fore-aft (FA) and side-to-side (SS) directions of the OWT may result in an underestimate of the maximum structural dynamic responses. Hence, this imparts the importance of considering ground motion directionality into account while analyzing the OWTs under seismic action. Moreover, design guideline available for the OWTs such as IEC 614000-1 (2005), DNVGL-ST-0437 (2016) recommend applying the response spectrum method in the seismic analysis of OWTs. However, the methodology for combining peak responses obtained from response spectrum analysis is not mentioned in the existing codes.

Floating wind turbines are widely regarded as seismically resilient, as seismic energy is not readily transferred from the seabed to the floating structure through mooring cables. This advantage is especially notable in spar and semisubmersible designs (Bhattacharya et al., 2021; James et al., 2022). In contrast, Tension Leg Platforms (TLPs) are more vulnerable to seismic events. The vertical component of an earthquake can alter the pretension in the mooring cables, which directly influences the platform's stability (Kawanishi et al., 1993; Chandrasekharan et al., 2006). A loss of cable pretension during vertical seismic shaking can lead to large overturning forces on the TLP, increasing the risk of platform failure (Bhattacharya et al., 2021). Apart from earthquake shaking, other secondary effects such as seaquakes, fault rupture, liquefaction, landslide etc. can affect the performance of floating structures. Bhattacharya et al. (2021) examined the impact of fault rupture on TLP under two scenarios: (i) the loss of the initial tension force and (ii) the increased tension caused by the foundation dragging in the tension leg. Their study identified the loss of pretension force is the most critical factor. Tsiapas et al. (2021) demonstrated that the factor of safety against pullout failure decreases significantly (0.1 to 0.2) during liquefaction but subsequently surpasses its initial value following the dissipation of excess pore water pressure. Additionally, anchor displacements were reported to remain within acceptable limits during liquefaction (Esef and Kaynia, 2019; Chaloulos et al., 2021). Kaynia et al. (2023) reported that that vertically propagating pressure waves in seawater, known as seaquakes, induced by vertical seabed motion, can result in the snap tension of tendons. Barron et al. (2024) found that the orientation of seismic loading has an impact on the displacement response of shared catenary anchors. The seismic vulnerability of floating wind turbines, particularly Tension Leg Platforms (TLPs), in conjunction with soil-structure interaction and the effects of vertical ground motion, has been largely overlooked in existing studies.

The characteristics of earthquake records vary based on the presence of pulses, frequency content, intensity measures, rupture distance, peak ground acceleration (PGA), peak ground velocity (PGV), and sustained maximum acceleration. To account for these uncertainties, a probabilistic approach is more effective in assessing potential damage from seismic loads. Seismic fragility analysis a powerful analytical tool for assessing probabilistic seismic performance of the structures (Kennedy et al. 1980). Various studies

have been performed seismic fragility analysis for buildings, bridges and offshore platforms (Ramamoorthy et al. 2006; Nielson and DesRoches et al. 2007; Ajamy et al. 2018). At present, few studies have been conducted to investigate the seismic fragility of the wind turbines (Kim et al. 2014; Mardfekri and Gardoni 2015; Cheng et al. 2023). Risi et al. (2018) showed that the monopile-supported OWTs are more vulnerable particularly to extreme crustal and interface earthquakes, and the vulnerability increases when the structure is supported by soft soil. Ali et al. (2020) investigated the seismic risk of 2 and 5 MW monopile supported OWTs subjected to pulse-like and non-pulse like records. The study showed that the 5 MW OWT is more vulnerable compared to 2 MW OWT for both pulse-like and non-pulse like records. Mo et al. (2021) developed seismic fragility curves of a 5MW monopile offshore wind turbine in operational and parked condition. Most of these studies have concentrated on monopile wind turbines. However, studies addressing uncertainty in seismic records through probabilistic seismic fragility analysis for Jacket and Floating wind turbines are limited.

This paper presents a comprehensive analysis of the seismic performance of both jacket-supported and TLP floating wind turbines. The study focused on checking the efficiency of percentage combination rule in predicting the seismic response of 10 MW jacket supported OWT under bi-directional earthquake components and discusses the effect of ground motion directionality on the critical responses obtained from time-history analyses. Furthermore, vulnerability assessment of floating structure is discussed in the subsequent session of the paper. The effect of pulse content on the seismic performance of 5 MW TLP is analyzed. Finally, the comparative study has been conducted to evaluate the seismic risk associated with the 10 MW jacketed and TLP floating OWTs by performing seismic fragility analysis through nonlinear time-history analysis (NTHA) under pulse and non-pulse earthquake motions.

NUMERICAL MODELLING

The numerical modelling of OWT supported by Jacket and Tension Leg Platform (TLP) are carried out in Abaqus CAE (2018). This study assess seismic responses only for 10 MW jacketed OWT (Nath and Haldar 2024), whereas both 5 MW Iberdrola (Oguz et al. 2018) and 10 MW Korean Institute of Energy Research (KIER) design (Madsen et al. 2020) is considered for TLP floating OWTs. The superstructure, including tower, jacket, and floating platform, is modelled as a beam element, while the piles are modeled as solid elements by providing equivalent stiffness. The rotor-nacelle assembly (RNA) is modelled as lumped mass and placed on the top of the tower. The three-dimensional solid elements (C3D8R) with Mohr coulomb constitutive model (e.g., Dai et al., 2020; Goh and Zhang 2017) are used to model soil. Boundary convergence study was carried out to fix the soil domain as 150 m × 150 m × 90 m, to avoid the any boundary reflection effect. The bottom of the soil domain is restrained in all directions, while the lateral boundaries are fixed in the horizontal direction and free to move in the vertical direction. The detailed modelling of OWT supported by jacketed foundation is mentioned in Nath and Haldar (2024). On the other hand, the truss elements modified with compression cut-off are provided for modelling the tendons for floating OWTs. The water is modelled by providing hydrostatic springs and viscous dampers. Assuming the platform to be a rigid body, the hydrostatic stiffness has been defined by the water plane area (A_{wp}), the overall centre of gravity (Z_G) and the centre of buoyancy (Z_B) from the water level (Bachynski & Moan, 2012). The initial pretension is applied in TLP by defining the buoyant force and gravity loading in the initial step. The schematic representation of the developed numerical model of 10 MW OWT supported by Jacket and TLP are provided in Figure 3.

VALIDATION OF NUMERICAL MODEL

To assess the reliability and accuracy of the proposed 3D numerical model, the first bending mode of tower and overall structural are compared with those reported by Borstel (2012) for 10 MW jacketed OWT and are shown in Table 1. The close agreement between the numerical predictions and the reference data serves to validate the accuracy of the developed model, thereby demonstrating its suitability for further analyses and predictive simulations in the context of structural dynamic behavior.

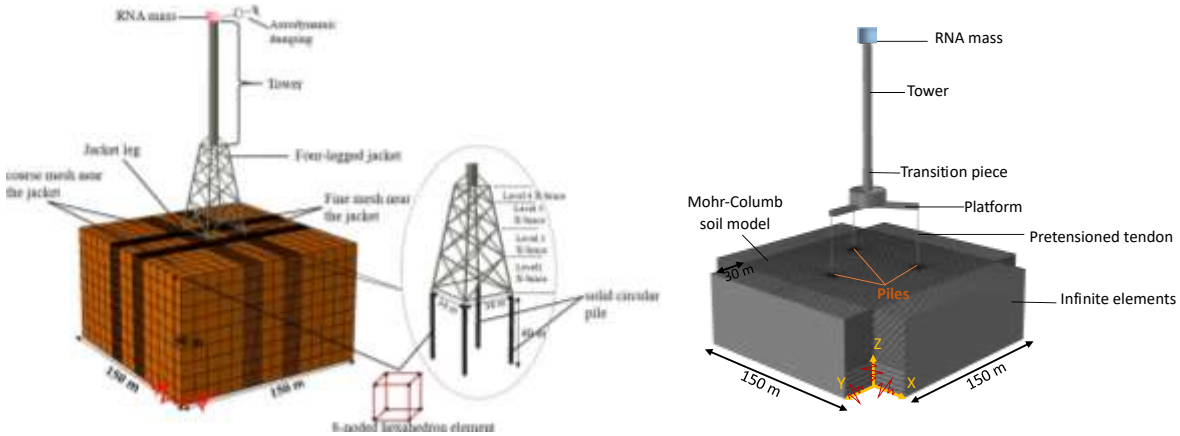

Fig. 3 Numerical model of 10 MW (a) jacket supported OWT subjected to bi-directional earthquake motions (Nath and Haldar 2024) (b) tension leg platform floating wind turbines developed in Abaqus CAE (2018)

Table 1a: Comparison of the natural frequency of the jacketed OWT

Structure	Mode	Present study (FE analysis) (Hz)	Reported value (Hz) (Borstel, 2012)
Tower	1st side-side bending	0.328	0.324
	1st fore-aft bending	0.330	0.327
Overall structure	1st side-side bending	0.259	0.286
	1st fore-aft bending	0.260	0.288

Table 1b: Validation of the 10MW TLP turbine model (Madsen et al., 2020) developed in Abaqus

Direction	Present study (FE analysis) (sec)	Reported (sec) (Madsen, 2020)
Surge/Sway	32.31	0.324
Pitch/Roll	3.772	3.77
Heave	1.305	1.3

SELECTION OF GROUND MOTION RECORDS

This study considers strong ground motion records selected from Pacific Earthquake Engineering Research Center (PEER) ground motion database. The selected suite includes near-field and far-field motions, characterized by both pulse and non-pulse types, comprising a total of 35 earthquake records. The rupture distance within 20 km from the fault is classified as near filed motion (Veggalam et al., 2021). The strong ground motions having magnitude (M) in the range of 6.5-7.6 are considered in this study. The peak ground acceleration (PGA) of the two components of the selected earthquakes lies in the range of 0.03g to 0.87g. The selected motions demonstrate a variety of spectral shape over a wide range of periods. The properties of selected ground motions are listed in Table 3.

PERCENTAGE COMBINATION RULE

In the first phase of analysis, the dynamic time-history analyses have been conducted considering various ground motion incidence angles. The peak responses then generated over all incident angles under bi-directional earthquake motions. In the second phase, response spectrum analysis is conducted and the peak response vectors $(\vec{R})$ are combined by percentage combination rule (Equation 1). A weighted percentage of 30% (AASTHTO 1996; Rosenblueth and Conteras 1977) and 40% (ATC 2003; Newmark

1975) is considered for percentage combination rule. The acceleration spectra of selected motions with 5% damping are given as input separately in the principal axis of the structure and then combined using the Equation 1. Modal superposition was carried out using complete quadratic combination approach (Khaled et al. 2011).

$$\vec{R} = \vec{R}_L + \alpha\vec{R}_T \quad (1a)$$

$$\vec{R} = \alpha\vec{R}_L + \vec{R}_T \quad (1b)$$

where, α is the weighted percentage (i.e., 0.3 and 0.4); $\vec{R}_L$ and $\vec{R}_T$ are the maximum response vectors resulting from the longitudinal and transverse components of earthquake motion acting separately along the two principal axes of the structure.

1. Analytical Methodology for Fragility Analysis

Seismic fragility is the likelihood of exceeding a defined damage state for a given intensity of earthquake motion (Kennedy 1994; Porter et al. 2007). Fragility functions can be generated through

Table 2: Properties of selected strong ground motions (PEER, 2024)

Sl. No	Earthquake Name	Year	Type	Record type	Magnitude
1	Anza	2001	Far Field	Non-Pulse	4.92
2	Central-Calif-02	1960	Near Field	Non-Pulse	5
3	Humbolt Bay	1937	Far Field	Non-Pulse	5.8
4	Whittier Narrows	1987	Far Field	Non-Pulse	5.99
5	Whittier Narrows	1987	Near Field	Non-Pulse	5.99
6	Northwest China	1997	Near Field	Non-Pulse	6.1
7	Superstition Hills-01	1987	Near Field	Non-Pulse	6.22
8	Coalinga	1983	Far Field	Non-Pulse	6.36
9	Imperial valley	1979	Near Field	Non-Pulse	6.53
10	Imperial Valley	1979	Near Field	Pulse	6.53
11	Northwest-California	1941	Far Field	Non-Pulse	6.6
12	Kobe Japan	1995	Near Field	Pulse	6.9
14	Loma Prieta	1989	Near Field	Pulse	6.93
15	Chi-Chi Taiwan	1999	Far Field	Pulse	7
16	Darfield, New Zealand	2010	Far Field	Pulse	7
17	Landers	1992	Far Field	Pulse	7.28
18	Taiwan Smart	1986	Far Field	Non-Pulse	7.3
19	Kocaeli	1999	Near Field	Pulse	7.51
20	Chi-Chi Taiwan	1999	Near Field	Pulse	7.62
21	Bhuj, India	2001	Far Field	Non-pulse	6.9
22	Chi-Chi, Taiwan-03	1999	Far Field	Non-pulse	6.2
23	Imperial Valley-06	1979	Near Field	Pulse-like	6.5
24	Imperial Valley-06	1979	Near Field	Pulse-like	6.5
25	Niigata, Japan	1964	Near Field	Pulse-like	7.5
26	Northridge-01	1994	Far Field	Non-pulse	6.7
27	Northridge-01	1994	Near Field	Pulse-like	7.6
28	Kocaeli, Turkey	1999	Near Field	Pulse-like	7.5
29	Loma prieta	1989	Near Field	Pulse-like	6.9
30	Kocaeli	1999	Near Field	Pulse-like	7.5
31	Irpinia	1980	Near Field	Pulse-like	6.9
32	Chi-Chi	1999	Near Field	Pulse-like	7.6
33	Chi-Chi	1999	Near Field	Pulse-like	7.6
34	Superstition Hills-02	1987	Near Field	Pulse-like	6.5
35	Kobe, Japan	1995	Far Field	Non-pulse	6.9

multiple methods, such as analytical, empirical, judgemental and hybrid approaches. However, analytical method is most commonly used approach in the area of OWTs to determine the seismic risk of the structures (Tran et al. 2020; Mo et al. 2021; Wang et al. 2024). An appropriate selection of intensity measure (IM) is needed to assess the seismic probabilities. The most commonly used IMs are peak ground acceleration (PGA), and spectral acceleration (Sa). This study considers PGA as IM value to define the seismic fragility function of the OWT. Incremental dynamic analysis is conducted via a number of nonlinear time history analyses by scaling the PGA from 0.1g to 1.5g with an increment of 0.1g for a selected set of earthquake motions. Assuming both the engineering demand parameters (EDP) and IM follow a logarithmic relationship, the fragility of OWT can be expressed as (Baker 2015):

$$P[EDP > ds_i \left| PGA \right] = \Phi\left[\frac{\ln(PGA/\xi)}{\sigma}\right] \quad (2)$$

where, $\Phi(.)$ is the standard normal distribution function; ξ and σ refers to the median and standard deviation of the fragility function. The damage probability is assessed based on a single damage state, defined by specific limit state conditions. Out of different engineering demand parameters considered, the tower-top drift in serviceability limit state (SLS) and von-mises equivalent stress in ultimate limit state (ULS) criteria is observed to be critical for Jacket while acceleration at nacelle and tower stress are considered for TLPs. The maximum allowable nacelle acceleration of 0.6g (Cheng et al. 2023), the permissible tower drift as 1.25 % of tower height (Asareh et al., 2016), and a yield strength of 266 MPa. The damage measures and their corresponding permissible limits are presented in Table 2.

Table 3: Defining damage states in SLS and ULS criteria for OWT

Limit states of OWT	Damage measures (DM)	Damage states (DS)
SLS	Nacelle acceleration	0.6 g
	Tower top drift	1.25 % of tower height
ULS	Von Mises stress-tower	266 MPa

RESULTS

1. Influence of Ground Motion Directionality on the Responses of OWT

The present study represents the peak responses obtained over various ground motion incidence angles (0º to 360º) for 10 MW jacketed OWT. Figure 4 depicts the demand to capacity ratio (Y) for the responses such as tower top displacement (u_{TT}), tower top rotation (θ_{TT}), mudline rotation (θ_{ml}), and bending moment (M_{tower}). The demand to capacity ratio is defined as the ratio of the maximum responses to the permissible limit of responses as mentioned in the available literature (Nath and Haldar 2024). It is observed that the peak displacement remains almost same for different incident angles and remains in the permissible limit over all indent angles of earthquake for all earthquake motion except for Niigata (1994) earthquake motion. It is also interesting to note that the normalized value of tower-top rotation (Y_{TTR}) for jacketed OWT is higher at the 90º and 120º angle of incidence for Bhuj (2001) and Imperial valley (1979) earthquake motion respectively. The study further noted that the Y_{TTR} exceeds the desirable limit for 120º angle of incidence for Imperial valley earthquake, but remains within the acceptable limits at 0º angle of incidence. The similar studies for Y_{ml} also shows that the demand to capacity ratio for the mudline rotation is maximum in other angle of incidences other than 0º angle of incidence for Bhuj (2001) and Niigata (1964) earthquake motion. However, the demand to capacity ratio for bending moment (Y_{BM}) remains in desirable limit state in all ground motion incidence angles. Therefore, the study highlights the significance of accounting for ground motion directionality when assessing the seismic responses of jacketed offshore wind turbines (OWTs).

2. Efficiency of Percentage Combination Rule

The adequacy of the percentage combination rule to predict the seismic demand of the OWT under bi-directional earthquake motions was examined (Nath and Haldar 2024). The values of engineering demand parameters (EDPs) of interest produced by percentage combination rule (30% and 40%) were compared with the maximum responses over all incident angles (i.e., 0º to 360º) computed by time-history analyses. The examined EDPs include tower top displacement (u_{TT}), tower top rotation (θ_{TT}), mudline rotation (θ_{ml}), and bending moment (M_{tower}). Under bi-directional orthogonal earthquake components, OWT

generates responses in the fore-aft and side-to-side directions for 0º to 360º angles of orientation. As the structural responses are recorded in the both fore-aft and side-side directions, the resultant of the response vectors is considered the peak response under the application of bi-directional earthquake components. Typical results of response parameters in terms of interacting tower top displacement, and tower-top rotation is depicted in Figures 5 and 6, which are generated based on the 30% combination rule and time history analysis for 10 MW jacket supported OWT. Similar studies were also conducted using the 40% combination rule, however, all results for the considered responses are not presented due to the brevity of the paper. The detailed responses are given in Nath and Haldar (2024). Moreover, the comparison between the maximum response over all incident angles and the corresponding response calculated by percentage rule is made in terms of relative error (RE).

$$RE(\%) = \frac{R_{max,i} - R_{max,TH}}{R_{max,TH}} \tag{3}$$

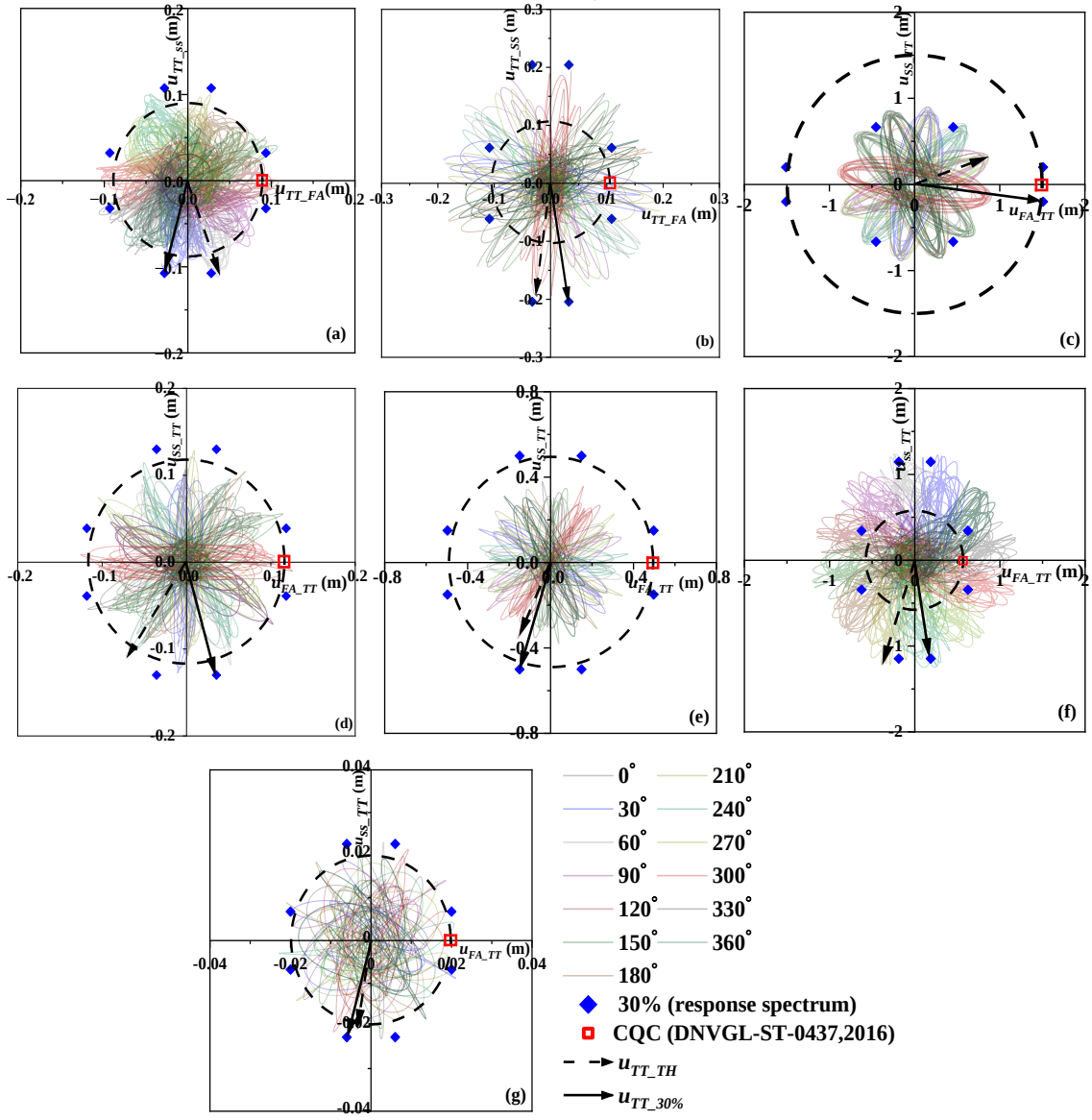

Fig. 5 Comparison of maximum resultant tower-top displacement vector u_{TH} and $u_{30\%}$ for (a) Bhuj (b) Chi-Chi (c) Imperial Valley (d) Kobe (e) Kocaeli (f) Niigata (g) Northridge earthquake motions

where R_i is the resultant responses computed from the percentage combination rule (i=30% and 40%) and R_{TH} is the maximum of the resultant responses computed from time-history analyses among all angles of incidence. Negative sign of RE indicates that the percentage combination rule yields an un-conservative response value while, positive sign refers conservative response value. Figure 7 demonstrates the REs in seismic responses calculated using percentage combination rules. The analysis indicates that both the 30% and 40% combination rules have a tendency to overestimate certain seismic responses of OWTs, such as tower top displacement, tower top rotation, and bending moment. In particular, the tower top displacement

and tower-top rotation overestimated by 3% to 24.6% in case of all considered earthquake motions, under the 30% combination rule (cf. Figure 7(a)). However, the responses are overestimated by maximum of 33% and 70% in case of Imperial Valley in 1979 and Kocaeli in 1999 earthquake motion respectively. On the other hand, for mudline rotation of the offshore wind turbine (OWT), the RE lies between 20% and -94.6%, when 30% combination rule is applied. Furthermore, as shown in Figure 7(a), the bending moment seem to be overestimated by 100% in case of Kocaeli (1999) earthquake motion. The results illustrated in Figure 7(b) indicates that the differences between the responses derived from the 40% combination rule and those obtained from time-history analysis in the presence of bi-directional earthquake motion are typically higher than those obtained with the 30% combination rule. However, the mudline rotation is better estimated by 40% combination rule with a maximum relative error of -65%. The findings suggest that the 30% combination rule provide better results than the 40% rule.

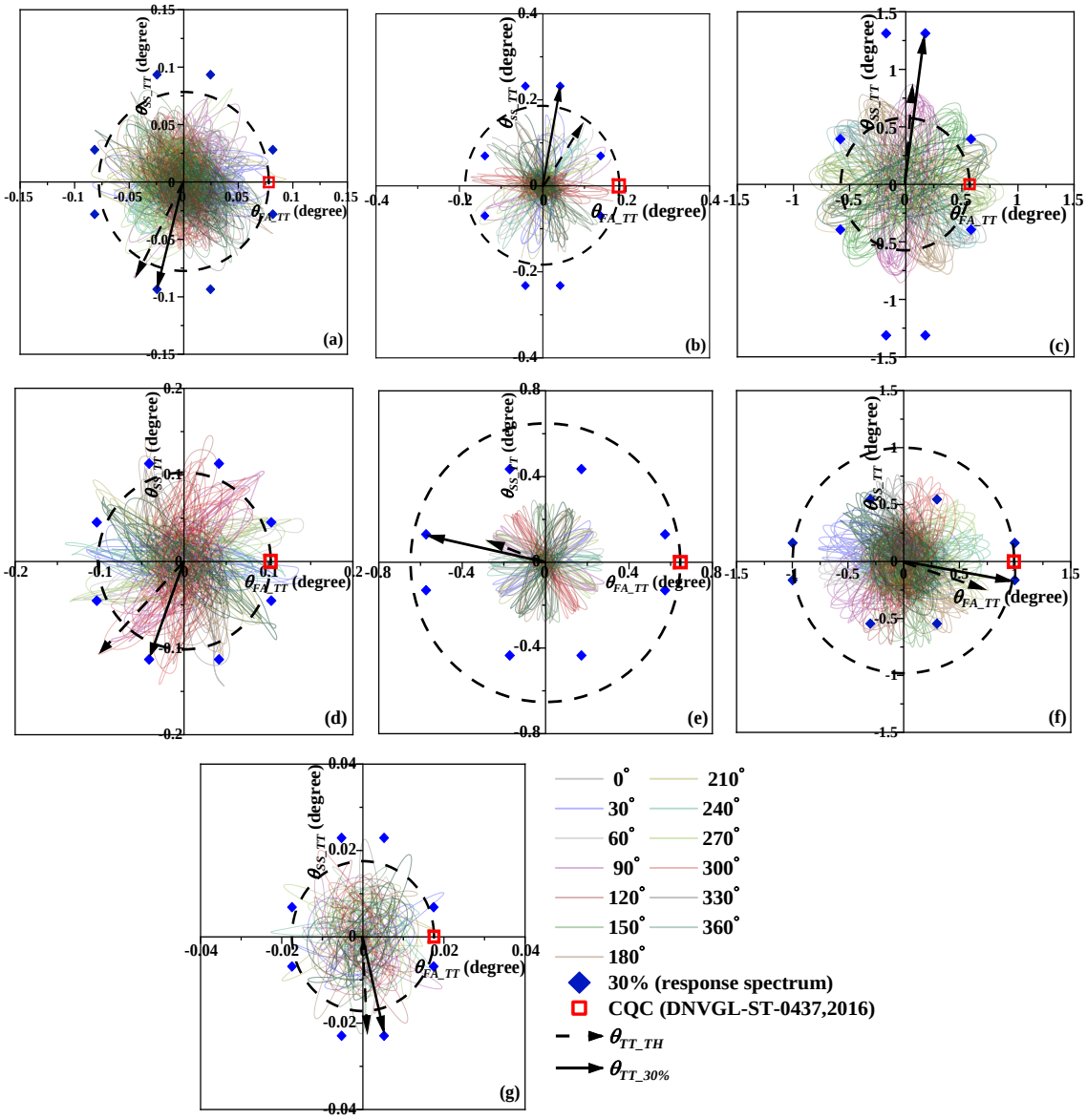

Fig. 6 Comparison of maximum resultant tower-top rotation vector θ_{TH} and $\theta_{30\%}$ for (a) Bhuj (b) Chi-Chi (c) Imperial Valley (d) Kobe (e) Kocaeli (f) Niigata (g) Northridge earthquake motions

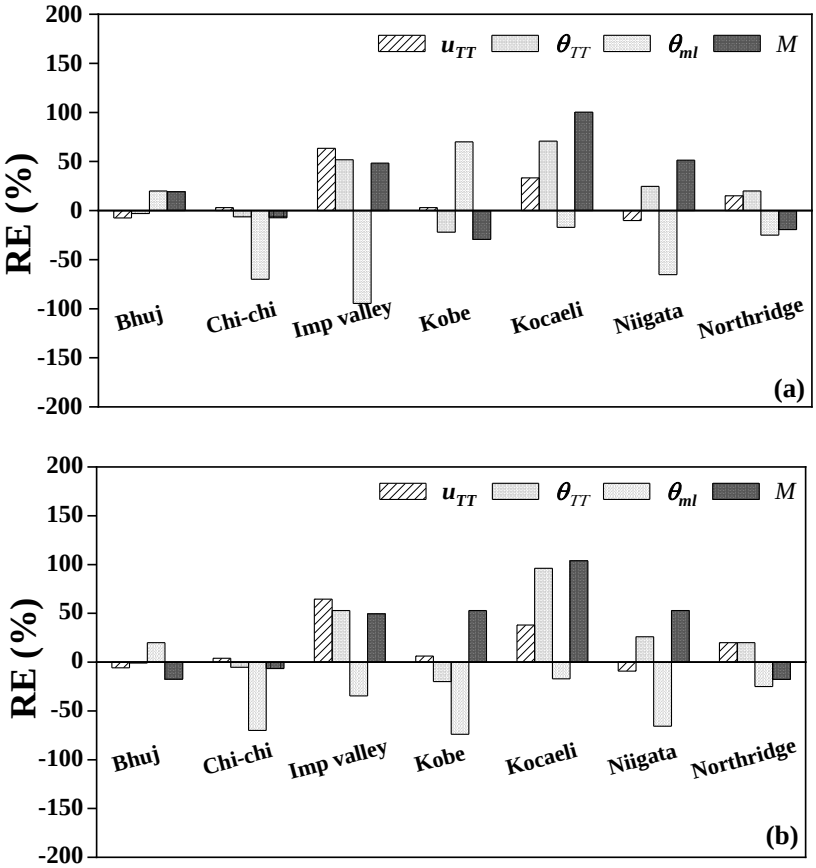

Fig. 7 RE of different EDPs between time-history and (a) 30% and (b) 40% combination rules

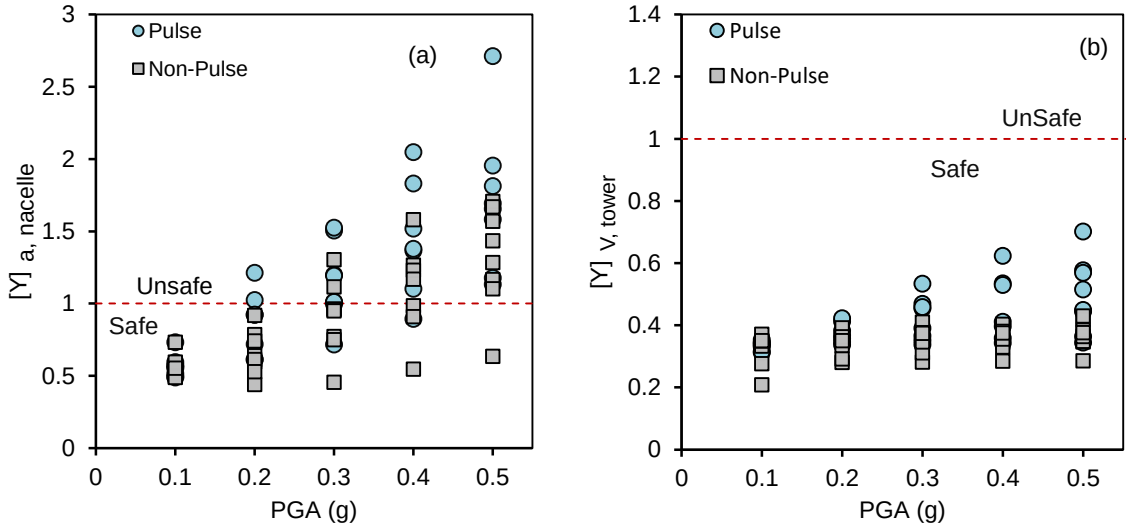

Fig. 8 Design parameters of TLP offshore wind turbine under combined seismic and environmental loads expressed in terms of demand by capacity ratio (a) acceleration at nacelle (SLS) (b)von Mises stresses at tower (ULS)

3. Seismic Response of TLP FOWT to Pulse and Non-Pulse Records

Seismic design considerations for jacket-supported offshore wind turbines indicate their vulnerability to seismic shaking. However, there is a limited number of available guidelines for floating wind turbines. Semisubmersible and spar-type floating wind turbines are generally considered as seismically resilient (James et al., 2022). On the other hand, Tension Leg Platform (TLP) wind turbines, which rely on highly pretensioned mooring lines for stability, may be affected by the vertical component of seismic events, potentially altering the pretension, and affecting platform stability (James and Haldar, 2024). Additionally,

there is a risk due to resonance caused by matching the predominant frequency of earthquake with natural frequency in the heave direction. Therefore, the seismic vulnerability of 5 MW and 10 MW TLP floating wind turbines are discussed in this session.

The seismic performance of 5 MW Iberdrola TLP wind turbine to pules and non-pulse records under combined seismic and environmental loading at parked condition are shown in Figure 8. The responses are presented in terms of capacity factor [Y] defined as the ratio of maximum demand occurred during an earthquake to the permissible limit or capacity. The acceleration at nacelle ($[Y]_{a,\ nacelle}$), and von mises stress in the tower ($[Y]_{V,\ tower}$), are the engineering demand parameters considered with PGA as the intensity measure. The structure is considered as unsafe when the demand exceeds the permissible limit (capacity factor > 1) (see Table 3). For all cases, given the same intensity level (i.e., PGA), earthquakes with pulse result in the maximum response. That is mainly because of the presence of large velocity pulses which has the predominant period falling in the frequency range of TLPs in heave direction. It is important to note that, despite scaling all earthquakes to the same intensity level, measured by Peak Ground Acceleration (PGA) from 0.1g to 1g, significant variations in responses are observed within the intensity level. Moreover, it is important to note that the variation in demand within the seismic records is increasing with increase in PGA highlighting the need for larger safety margins in high seismic risk areas. The variation can be due to the inherent uncertainty within the seismic record attributed due to the variation in properties such as peak ground velocity, predominant frequency, presence of velocity pulses, sustained maximum acceleration, mean period of the earthquake, arias intensity, spectral acceleration, cumulative absolute velocity, earthquake magnitude, rupture distance, etc. Moreover, this large uncertainty within the same intensity measure suggest to conduct a more comprehensive performance evaluation like seismic fragility analysis which accounts for the variability in earthquake ground motions by using a probabilistic framework.

4. Fragility Analysis of Jacket and TLP

Incremental dynamic analysis (IDA) is conducted for different EDPs to develop the fragility curves by considering PGA as the intensity measure. Figure 9 shows the comparison between the fragility curves derived for damage states corresponding to SLS and ULS criteria for 10 MW jacket and 10 MW TLP KIER floating wind turbines. According to Indian standard seismic code (IS 1893) for the Gujarat region, a minor

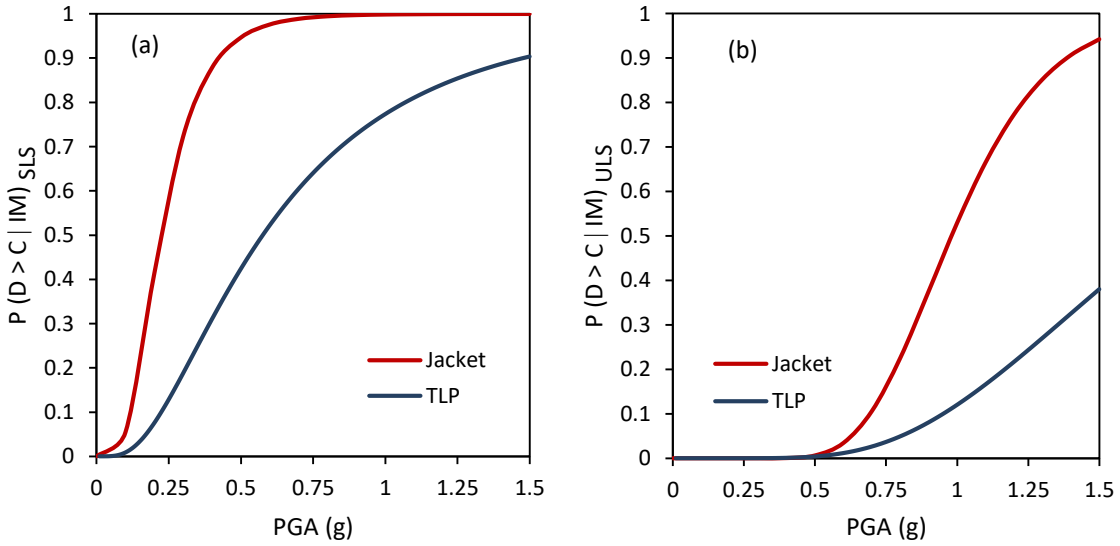

Fig. 9 Fragility curves developed for 10 MW Jacket and TLP under different damage states for (a) SLS and (c) ULS criteria

earthquake is classified with a peak ground acceleration (PGA) of 0.1g, the design basis earthquake (DBE) with 0.18g, and the maximum considered earthquake (MCE) with 0.36 g. In both SLS and ULS, jacket shows higher vulnerability compared to TLP floating wind turbine. For a DBE, the probability of damage is 81% in Jacket whereas, it is only 26% for TLP in SLS. In ULS, the jacket shows considerable damage probability at high-intensity earthquake with PGA greater than 1g while the probability of failure remains less than 10% in TLP. Hence, TLPs are observed to be a viable option over Jacket in seismically vulnerable areas at intermediate water depth.

CONCLUSIONS

This paper examines the seismic performance of both bottom-fixed and floating wind turbines under multi-directional earthquake motions. It compares the efficiency of the percentage combination rule using response spectrum analysis with time history analysis that accounts for ground motion directionality. Additionally, a fragility analysis is conducted to assess the seismic risk of Jacket and TLP floating offshore wind turbines. The key findings are summarized as follows:

1) Elastic demand parameters, such as tower-top and mudline rotation, show significant variation at orientation angles other than the 0° incidence angle of earthquake motions. However, the maximum mudline rotation response is underestimated by 2% to 69% across all selected motions. This highlights the importance of analyzing responses at various earthquake incidence angles to ensure structural integrity under seismic loading.
2) The 30% combination rule generally provided accurate predictions for peak responses, such as tower-top displacement and rotation, with maximum errors of 15% and 22% in most earthquake cases examined in this study. However, mudline rotation was more accurately estimated using the 40% combination rule compared to the 30% rule.
3) The vulnerability of Jacket-supported offshore wind turbines (OWTs) under the Serviceability Limit State (SLS) criteria is primarily influenced by tower-top drift response, rather than von Mises stress under the Ultimate Limit State (ULS) criteria. This results in a comparatively higher probability of exceedance, even at a high peak ground acceleration (PGA) level of 0.36g, for slight, moderate, and severe damage states.
4) Tension leg platforms (TLPs) are more susceptible to pulse-like seismic records compared to non-pulse records, primarily due to significant velocity pulses. The standard deviation from the mean response increases with increasing peak ground acceleration (PGA), indicating the need for higher safety margins in seismic regions. Nacelle acceleration is identified as the primary failure mode, with the probability of rotor-nacelle assembly (RNA) damage reaching 0.9 at a PGA of 1.5 g.
5) Seismic vulnerability assessments reveal that jacket structures are more susceptible to seismic shaking than Tension Leg Platform (TLP) floating wind turbines. The inherent flexibility and motion capacity of floating wind turbines enable them to absorb and adapt to seismic forces more effectively, thereby reducing the risk of structural damage. Consequently, floating wind turbines represent a promising alternative for deployment in seismically active regions, providing enhanced safety, structural stability, and long-term operational viability compared to traditional fixed-bottom designs.

REFERENCES

1. Ajamy, A., Asgarian, B., Ventura, C.E. and Zolfaghari, M.R. (2018). “Seismic Fragility Analysis of Jacket Type Offshore Platforms Considering Soil-Pile-Structure Interaction”, *Eng. Struct.*, Vol. 174, pp. 198–211.
2. Alati, N., Failla, G. and Arena, F. (2015). “Seismic Analysis of Offshore Wind Turbines on Bottom-Fixed Support Structures”, *Philos Trans R Soc A Math Phys Eng Sci.*, Vol. 373, No. 2035, pp. 20140086.
3. Ali, A., Risi, R. De., Sextos, A., Goda, K. and Chang, Z. (2020). “Seismic Vulnerability of Offshore Wind Turbines to Pulse and Nonpulse Records”, *Earthquake Eng. Struct. Dyn.,* Vol. 49, No. 1, pp. 24–50.
4. Asareh, M.A., Schonberg, W. and Volz, J. (2016). “Fragility Analysis of a 5-MW NREL Wind Turbine Considering Aero-Elastic and Seismic Interaction Using Finite Element Method”, *Finite Elem. Anal. Des.* Vol. 120, pp. 57–67.
5. ASCE, (1986). “Seismic Analysis of Safety-Related Nuclear Structures and Commentary on Standard for Seismic Analysis of Safety Related Nuclear Structures”, *ASCE 4-86, New York: ASCE*.
6. ASCE, (2016). “Minimum Design Loads and Associated Criteria for Buildings and other Structures”, *ASCE/SEI 7-16. Reston, VA: ASCE*.
7. Athanatopoulou, A.M. (2005). “Critical Orientation of Three Correlated Seismic Components”, *Engineering Structures*, Vol. 27, pp. 301-312.

8. Basu, S. and Shinozuka, M. (2011). "Effect of Ground Motion Directionality on Fragility Characteristics of a Highway Bridge", *Advances in Civil Engineering*.
9. Bhattacharya, S. and Goda, K. (2016). "Use of Offshore Wind Farms to Increase Seismic Resilience of Nuclear Power Plants", *Soil Dyn Earthq Eng*., Vol. 80, pp. 65-8.
10. Bhattacharya, S., Nikitas, G., Arany, L. and Nikitas, N. (2017). "Soil-Structure Interactions for Offshore Wind Turbines", *IET Eng Technol Ref*.
11. Chaloulos, Y.K., Tsiapas, Y.Z. and Bouckovalas, G.D. (2021). "Seismic Analysis of a Model Tension Leg Supported Wind Turbine under Seabed Liquefaction", *Ocean Engineering*, Vol. *238*, pp. 109706.
12. Cheng, Y., Luo, Y., Wang, J., Dai, K. and Wang, W. (2023). "Fragility and Vulnerability Development of Offshore Wind Turbines under Aero-Hydro Loadings", *Eng. Structures*, Vol. 293, pp. 116625.
13. De, Risi R., Bhattacharya, S. and Goda, K. (2018). "Seismic Performance Assessment of Monopile-Supported Offshore Wind Turbines Using Unscaled Natural Earthquake Records", *Soil Dyn Earthq Eng*, Vol. 109, pp. 154–72.
14. DNV-OSJ101, (2014). "Design of Offshore Wind Turbine Structures", *Hovik, Denmark: Det Norske Veritas*.
15. DNVGL-ST-0126 (Det Norske Veritas), (2016). "Design of Offshore Wind Turbine Structures", *Hovik, Denmark: DNV*.
16. GL. (Germanischer Lloyd), (2010). "Guideline for the Certification of Wind Turbines", *Hamburg: Germany: GL*.
17. Heredia-Zavoni, E. and Machicao-Barrionuevo, R. (2004). "Response to Orthogonal Components of Ground Motion and Assessment of Percentage Combination Rules", *Earthquake Eng. Struct. Dyn*., Vol. 33, No. 2, pp. 271–284.
18. Hovind, E. and Kaynia, M. (2014). "Earthquake Response of Wind Turbine with Non-Linear Soil-Structure Interaction", *In proceedings of 9th International conference on Structural Dynamics, EURODYN*, pp. 623-630.
19. IEC 61400–3. wind turbines Part3, (2009). "Design Requirements for Offshore Wind Turbines", *Switz: Int Electrotech Comm Geneva*.
20. IEC 61400–3. wind turbines Part1, (2005). "Design Requirements for Offshore Wind Turbines", *Switz: Int Electrotech Comm Geneva*.
21. IS 1893. Part 1, (2016), "Criteria for Earthquake Resistant Design of Structures", *Bureau of Indian Standards", New Delhi, India*.
22. James, M. and Haldar, S. (2022). "Seismic Vulnerability of Jacket Supported Large Offshore Wind Turbine Considering Multi-Directional Ground Motions", *Structures*, 43:407-423.
23. James, M., Haldar, S. and Bhattacharya, S. (2022. "December). Seismic Response of Spar Floating Offshore Wind Turbine", *In Indian Geotechnical Conference*, pp. 331-341. Singapore: Springer Nature Singapore.
24. James, M. and Haldar, S. (2021). "Seismic DESIGN of Large Offshore Wind Turbine Considering Rocking Vibration", *In Transportation, Water and Environmental Geotechnics: Proceedings of Indian Geotechnical Conference 2020*, Vol. 4, pp. 411-422. Springer Singapore.
25. James, M. and Haldar, S. (2024). "Design Strategies of Offshore Wind Turbines in Shallow and Deep Water-Indian Perspective", *Indian Geotechnical Journal*, pp. 1-16.
26. Ju, S. and Huang, Y. (2019). "Analyses of Offshore Wind Turbine Structures with Soil-Structure Interaction under Earthquakes", *Ocean Eng.* Vol. 187, pp. 106190.
27. Kalkan, E. and Kwong, N.S. (2013). "Pros and Cons of Rotating Ground Motion Records to Fault-Normal/Parallel Directions for Response History Analysis of Buildings", Journal of Structural Engineering, Vol. 140, No. 3.
28. Kaynia, A.M. (2019). "Seismic Considerations in Design of Offshore Wind Turbines", *Soil Dyn Earthq Eng.* Vol. 124, pp. 399–407.

29. Kennedy, R.P., Cornell, C.A., Campbell, R.D., Kalpan, S. and Perla, H.F. (1980). "Probabilistic Seismic Safety Study on an Existing Power Plant", *Nucl. Eng. Des.*, Vol. 59, No. 2, pp. 315-338.
30. Khaled, A., Tremblay, R. and Massicotte, B. (2011). "Effectiveness of the 30%-Rule at Predicting the Elastic Seismic Demand on Bridge Columns Subjected to Bi-Directional Earthquake Motions", *Eng. Struct.*, Vol. 33, No. 8, pp. 2357–2370.
31. Kim, D.H., Lee, G. and Lee, I.K. (2014). "Seismic Fragility Analysis of 5 MW Offshore Wind Turbine", *Renew Energy*, Vol. 65, pp. 250–6.
32. MacRae, G.A. and Mattheis, J. (2000), "Three-Dimensional Steel Building Response to Near-Fault Motions", *J. Struct. Eng.*, Vol. 126, No. 1, pp. 117–126.
33. Madsen, F.J., Nielsen, T.R.L., Kim, T., Bredmose, H., Pegalajar-Jurado, A., Mikkelsen, R.F. and Shin, P. (2020). "Experimental Analysis of the Scaled DTU10MW TLP Floating Wind Turbine with Different Control Strategies", *Renewable Energy*, Vol. 155, pp. 330-346.
34. Maleki, S. and Bisadi, V. (2006). "Orthogonal Effects in Seismic Analysis of Skewed Bridges", *J. Bridge Eng.* Vol. 11, No. 1, pp. 122–130.
35. Mo, R., Cao, R., Liu, M. and Li, M. (2021). "Effect of Ground Motion Directionality on Seismic Dynamic Responses of Monopile Offshore Wind turbines", *Renew Energy*, Vol. 175, pp. 179–99.
36. Nath, U. and Haldar, S. (2024). "Effectiveness of Combination Rule at Predicting the Elastic Seismic Demand of Jacket-Supported Offshore Wind Turbine Subjected to Bi-Directional Motions", *Structures*, Vol. 64, pp. 106455.
37. Nath, U. and Haldar, S. (2023). "Seismic Fragility Analysis of Jacket Supported Offshore Wind Turbine Considering Ground Motion Directionality", *In Offshore Site Investigation Geotechnics 9th International Conference Proceeding*, Vol. 1168, No. 1173, pp. 1168-1173. Society for Underwater Technology.
38. Nielson, B.G. and DesRoches, R. (2007). "Seismic Fragility Methodology for Highway Bridges using a Component Level Approach", *Earthq. Eng. Struct. Dynam*, Vol. 36, No. 6, pp. 823–839.
39. Oguz, E., Clelland, D., Day, A.H., Incecik, A., López, J.A., Sánchez, G. and Almeria, G.G. (2018). "Experimental and Numerical Analysis of a TLP Floating Offshore Wind Turbine", *Ocean Engineering*, Vol. 147, pp. 591-605.
40. Prowell, I., Elgamal, A., Uang, C.M., Enrique Luco, J., Romanowitz, H. and Duggan, E. (2014). "Shake Table Testing and Numerical Simulation of a Utility-Scale Wind Turbine including Operational Effects", *Wind Energy*, Vol. 17, No. 7, pp. 997-1016.
41. Patil, A., Jung, S. and Kwon, O.S. (2016). "Structural Performance of a Parked Wind Turbine Tower Subjected to Strong Ground Motions", *Engineering Structures*, Vol. 120, pp. 92-102.
42. Patra, S.K. and Haldar, S. (2020). "Fore-Aft and the Side-To-Side Response of Monopile Supported Offshore Wind Turbine in Liquefiable Soil", *Mar. Georesources Geotechnology.*, Vol. 39, No. 12, pp. 1411–32.
43. Patra, S.K. and Haldar, S. (2021a). "Long-Term Drained and Post-Liquefaction Cyclic Behaviour of Offshore Wind Turbine in Silty Sand Using Element Tests", *Arabian J. Sci. Eng.*, Vol. 46, No.5, pp. 4791-4810.
44. Patra, S.K. and Haldar, S. (2021b). "Seismic Response of Monopole Supported Offshore Wind Turbine in Liquefiable Soil", *Structures*, Vol. 31, pp. 248-265.
45. Sapountzakis, E.J., Dikaros, I.C., Kampitsis, A.E. and Koroneou, A.D. (2015). "Nonlinear Response of Wind Turbines under Wind and Seismic Excitations with Soil–Structure Interaction", *J. Comput. Nonlinear Dynam.*, Vol. 10, No. 4, pp. 41001-41007.
46. Sharmin, F., Hussan, M., Kim, D. and Cho, S.G. (2017). "Influence of Soil-Structure Interactions on Seismic Responses of Offshore Wind Turbine Considering Earthquake Incident Angle", *Earthquakes and Structures*, Vol. 13, pp. 39-50.
47. Tran, T., Hussan, M., Kim, D. and Nguyen, P. (2020). "Distributed Plasticity Approach for the Nonlinear Structural Assessment of Offshore Wind Turbine", *Int. J. Naval Arch. Ocean Eng.*, Vol. 12, pp. 743–754.
48. Wang, L. and Dong, X.T. (2011). "Influence of Earthquake Directions on Wind Turbine Tower under Seismic Action", *Adv. Mater. Res., Vol.* 243–249, pp. 3883–3888.

49. Zhao, X. and Maißer, P., (2006). "Seismic Response Analysis of Wind Turbine Towers including Soil-Structure Interaction", *Proc Inst Mech Eng Part K J Multi-Body Dyn.,* Vol. 220, No. 1, pp. 53–61.
50. Zheng, X.Y., Li, H., Rong, W. and Li, W. (2015). "Joint Earthquake and Wave Action on the Monopile Wind Turbine Foundation: an Experimental Study", *Mar Struct*, Vol. 44, pp. 125-41.